Measurement of the percolation threshold for fully penetrable disks of different radii

J. Quintanilla*

Department of Mathematics, University of North Texas, Denton, Texas 76203
(Received 3 November 2000; published 23 May 2001)

We perform simulations of gradient percolation to study the percolation threshold for systems of homogeneous fully penetrable disks of variable radii. We find that, if the radii follow a uniform distribution, the percolation threshold is $0.686\,610 \pm 0.000\,007$. We also investigate binary dispersions, studying the influence of constitutive parameters on the percolation threshold and suggesting an empirical formula for the threshold. We find that, with the appropriate parameters, a percolation threshold of approximately 0.76 can be achieved. The minimal threshold of $0.676\,339 \pm 0.000\,004$ is achieved by disks of equal radius.

I. INTRODUCTION

Measurement of the percolation threshold for fully penetrable disks has received much attention in the literature. In this paper, we define the percolation threshold to be the probability that a randomly chosen point is covered by a disk; this quantity has also been called the covered volume fraction. Techniques using spatial statistics have been proposed for the theoretical prediction of percolation thresholds [1]; the purpose of the present work is efficient measurement of the threshold via simulations. For disks of equal radius, the threshold has recently been measured to be $\phi_c = 0.676\,339 \pm 0.000\,004$ [2]. This value was found by using gradient percolation, a technique that simulates disks that are centered on the points of an underlying inhomogeneous Poisson field [3]. The percolation threshold was then computed by measuring the average location of the frontier, or the edge of the percolating cluster that naturally forms [4]. The frontier was found using two different efficient techniques: the gap-traversal method and the frontier-walk method, previously used for lattice systems [5].

While much attention has been given to fully penetrable disks of equal size, relatively little study has been undertaken for analogous percolation problems for systems of disks with different radii. Monte Carlo studies have shown that the percolation threshold for polydispersed disks is different than that of monodispersed disks [6,7]. However, these studies made no attempt to study the nature of the threshold's dependence on the underlying distribution of radii. More recently, the existence of a binary dispersion with a higher percolation threshold than for monodispersed disks has been mathematically proven; it has also been conjectured that the monodisperse distribution minimizes the percolation threshold [8].

In the present paper, we use gradient percolation to study the percolation threshold for two different systems of fully penetrable disks with variable radii. In both systems, our results add two decimal places to previous estimates of the percolation thresholds. In Sec. II, we consider the percolation threshold ϕ_c^{uniform} for disks whose radii follow a uniform distribution on $[0,R]$, where R is the maximum permitted

radius [7]. In Sec. III, we investigate the percolation threshold $\phi_c(f,\lambda)$ of binary dispersions of disks with two different radii R and λR, where $0 \leq \lambda \leq 1$ and f is the fraction of disks with the smaller radius λR. We also develop an empirical formula for $\phi_c(f,\lambda)$ that reasonably fits our data. Finally, we investigate the accessible part of the frontier and find that binary dispersions exhibit the Grossman-Aharony effect in the same manner as equal-sized disks.

II. UNIFORMLY DISTRIBUTED RADII

In this section, we study the percolation threshold of disks of variable radii when the radii R_i are chosen to follow a uniform distribution; that is,

$$\text{Prob}(R_i = x)\,dx = \begin{cases} dx/R & 0 \leq x \leq R \\ 0 & \text{otherwise,} \end{cases} \quad (1)$$

where R is the largest permitted radius. To do so, we will simulate within a unit square an underlying inhomogeneous Poisson field and independently place disks of random radius on the points of this Poisson field. Following Ref. [2], we do not simulate regions for all possible particle volume fractions ϕ but only in a prescribed range

$$\phi_{\min} < \phi < \phi_{\max}, \quad (2)$$

where $\phi_{\min}$ and $\phi_{\max}$ are so chosen that the simulated frontier lies between these values. We also define the *effective system length* as

$$\ell = \frac{L}{R(\phi_{\max} - \phi_{\min})}. \quad (3)$$

This dimensionless parameter ℓ is the inverse of the gradient of ϕ, measured in terms of the maximum disk radius R and the length $L=1$ of the unit square. The effective system length is analogous to the lattice size of a lattice system.

We choose a linear variation in the particle volume fraction within the unit square; that is,

$$\phi(x) = (1-x)\phi_{\min} + x\phi_{\max}. \quad (4)$$

To achieve this, we recall that, for homogeneous systems [3], the particle volume fraction is given by

*Electronic address: johnq@unt.edu

$$\phi = 1 - e^{-\pi\rho M_2}, \tag{5}$$

where ρ is the number density of the disks and M_2 is the second moment of the distribution of radii. In the present problem, using Eq. (1),

$$\phi = 1 - e^{-\pi\rho R^2/3}. \tag{6}$$

Therefore, if R is sufficiently small [9], a linear variation may be obtained by choosing

$$\rho(x) = \frac{-3\ln[(1-x)\phi_{\min} + x\phi_{\max}]}{\pi R^2} \tag{7}$$

to be the number density of the underlying inhomogeneous Poisson field.

The details of the frontier-walk method are given elsewhere [2]. During the simulations, the frontier-walk method of Ref. [2] was used to identify the frontier. Systems with $3000 \leq \ell \leq 50\,000$ were simulated on a 400-MHz microcomputer with 128 MB of RAM. For each simulation, the percolation threshold was measured in two different ways. First, the average location of the frontier $\phi_c^{(1)}(\ell)$ was computed using an expression given elsewhere [4]. (This quantity was simply called p in this reference.) Second, and more simply, the average location $\phi_c^{(2)}(\ell)$ of the *centers* of the disks on the frontier was computed. These two estimates were obtained simultaneously in the simulations. On intuitive grounds, these two averages are both expected to converge to the actual percolation threshold as the effective system length ℓ increases, and the numerical evidence for such convergence is quite compelling. However, a rigorous proof of this convergence has yet to be found.

For $3000 \leq \ell \leq 50\,000$, we calculated $\phi_c^{(1)}(\ell)$ and $\phi_c^{(2)}(\ell)$ with an error tolerance of 1×10^{-5}. To obtain this accuracy using a 400-MHz microcomputer, roughly 125 to 200 h were required to generate and measure the 6 to 10 billion frontier arcs for each displayed value of ℓ. Larger values of ℓ required greater computational effort. In full, a total of 53 billion arcs were generated over 6 weeks of computer time.

In Fig. 1, we present $\phi_c^{(1)}(\ell)$ and $\phi_c^{(2)}(\ell)$, the individual error bars for each measurement, and their regression lines as functions of $1/\ell$. We see that, for sufficiently large ℓ, the observed values of both $\phi_c^{(1)}(\ell)$ and $\phi_c^{(2)}(\ell)$ appear to vary linearly with $1/\ell$. Using a regression fit for the data, we also find that the y intercepts of the two regression lines differ, not surprisingly, by an amount of the order of the size of the error bars. Taking the average of these two y intercepts, we estimate the percolation threshold for fully penetrable disks with uniformly distributed radii to be

$$\phi_c^{\text{uniform}} = 0.686\,610(7), \tag{8}$$

which corresponds to

$$\rho_c^{\text{uniform}} R^2 = 1.108\,010(7) \tag{9}$$
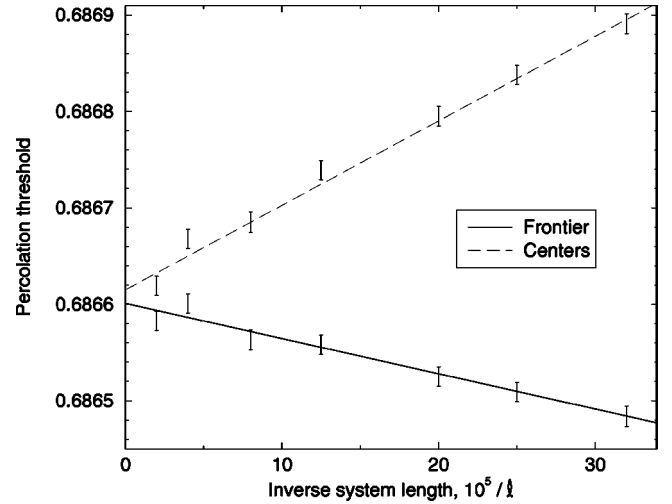
FIG. 1. Estimates of the percolation threshold, as a function of $1/\ell$, for disks whose radii follow a uniform distribution. The bars show the estimated error of 10^{-5} for each measurement. The lower line shows the estimates $\phi_c^{(1)}(\ell)$, obtained from the average location of the frontier, while the upper line shows the estimates $\phi_c^{(2)}(\ell)$, obtained from the average location of the centers of the disks comprising the frontier. Regression fits to both sets of data are in agreement within the given error tolerance, and the two y intercepts only differ by approximately this error tolerance.

in terms of the dimensionless number density. We note that two extra decimal places of accuracy have been added to the previous estimate of $\phi_c^{\text{uniform}} = 0.6860(12)$ [7].

In these evaluations, the number in parenthesis represents the error tolerance (one standard deviation) in the last digit. These error estimates are found by using the errors of the individual measurements and computing the variance of the y intercept in the regression model [10], which we now briefly describe. Suppose a set of points $\{(x_i, Y_i)\}$ are given, where the x_i are known but the Y_i are random variables with a given mean y_i and standard deviation σ. Then the expected value of the y intercept of the regression line may be found using the ordinary regression model using the points $\{(x_i, y_i)\}$, while the variance of the y intercept is given by

$$\frac{\sigma^2 \sum x_i^2}{\sum x_i^2 - \left(\sum x_i\right)^2}. \tag{10}$$

This formula was previously applied to determine the error of the percolation threshold equal-sized disks [2]. We note that, as a consequence of Eq. (10), the error estimate 7×10^{-6} for the percolation threshold is slightly smaller than the error estimate 1×10^{-5} associated with each individual measurement of $\phi_c^{(1)}(\ell)$ and $\phi_c^{(2)}(\ell)$.

As a further check of our simulations, we also compute the fractal exponents for the perimeter P and the width σ of the frontier as a function of ℓ. Expressions for these quantities may be found in [4]. We find that, within the tolerances

TABLE I. Estimates of the percolation threshold $\phi_c(f,\lambda)$ for binary dispersions of fully penetrable disks, where f is the fraction of smaller disks and $\lambda < 1$ is the ratio of the two radii. Each value has an estimated error of 5 in the last decimal place. All values are larger than $\phi_c \approx 0.676\,339$, which is both the percolation threshold for disks of equal size and also the value of $\phi_c(f,\lambda)$ for $f=0$ and $f=1$.

	$f=0.1$	$f=0.2$	$f=0.3$	$f=0.4$	$f=0.5$	$f=0.6$	$f=0.7$	$f=0.8$	$f=0.85$	$f=0.9$
$\lambda=0.1$	0.67658	0.67693	0.67727	0.67785	0.67856	0.67973	0.68161	0.68525	0.68877	0.69542
$\lambda=0.2$	0.67706	0.67796	0.67917	0.68052	0.68261	0.68557	0.69013	0.69798	0.70450	0.71429
$\lambda=0.3$	0.67751	0.67893	0.68061	0.68275	0.68548	0.68912	0.69417	0.70119	0.70541	0.70849
$\lambda=0.4$	0.67777	0.67928	0.68112	0.68326	0.68593	0.68896	0.69262	0.69607	0.69695	0.69601
$\lambda=0.5$	0.67762	0.67903	0.68075	0.68245	0.68438	0.68640	0.68809	0.68892	0.68843	0.68679
$\lambda=0.6$	0.67742	0.67858	0.67968	0.68085	0.68206	0.68285	0.68338	0.68317	0.68251	0.68136
$\lambda=0.7$	0.67705	0.67768	0.67846	0.67899	0.67960	0.67986	0.68002	0.67946	0.67908	0.67841
$\lambda=0.8$	0.67675	0.67713	0.67728	0.67762	0.67780	0.67778	0.67774	0.67754	0.67728	0.67696
$\lambda=0.9$	0.67639	0.67656	0.67668	0.67662	0.67666	0.67661	0.67670	0.67652	0.67659	0.67658

of simulation, $P \propto \ell^{3/7}$ and $\sigma \propto \ell^{-3/7}$. These same exponents were found in previous work for equal-sized disks [2] and on the lattice [11,12].

III. BINARY DISPERSIONS

We now consider the percolation threshold $\phi_c(f,\lambda)$ for binary dispersions. In these systems, the radii R_i of the disks can be either λR or R with probabilities f and $1-f$:

$$\text{Prob}(R_i = x) = \begin{cases} f & x = \lambda R \\ 1-f & x = R. \end{cases} \qquad (11)$$

Once again, the largest permitted radius is R, and so we require $0 \le \lambda \le 1$. We also note that $0 \le f \le 1$. The radii are assigned independently of each other and the underlying inhomogeneous Poisson field. We also note the obvious boundary conditions on $\phi_c(f,\lambda)$,

$$\phi_c(0,\lambda) = \phi_c(1,\lambda) = \phi_c(f,0) = \phi_c(f,1) \equiv \phi_c, \qquad (12)$$

where ϕ_c is the percolation threshold for equal-sized disks. (The degenerate case $f=1, \lambda=0$ is obviously not considered in the above boundary conditions.)

A. Simulation results

In simulating binary dispersions, we again specify a linear variation of the particle volume fraction $\phi(x)$. To do this, we note that, for homogeneous binary dispersions,

$$\phi = 1 - \exp\{-\rho \pi R^2 [f \lambda^2 + (1-f)]\} \qquad (13)$$

from Eq. (5), and so we choose

$$\rho(x) = \frac{-\ln[(1-x)\phi_{\min} + x\phi_{\max}]}{\pi R^2 [f\lambda^2 + (1-f)]}. \qquad (14)$$

As before, the simulated values of $\phi_c^{(1)}(\ell)$ and $\phi_c^{(2)}(\ell)$ are used to estimate the true percolation threshold. However, because we wish to study the behavior of $\phi_c(f,\lambda)$ over many values of both f and λ, less computational effort is expended to measure the two estimates than in the previous section. We choose to measure these two estimates with an error of

5×10^{-5}. With this larger error tolerance, the error bars on $\phi_c^{(1)}(\ell)$ and $\phi_c^{(2)}(\ell)$ will actually *overlap* for large values of ℓ. As a result, we cannot expect linear regression over multiple values of ℓ to provide much improvement in estimating the true percolation threshold. Furthermore, based on Fig. 1, the difference of the *average* of the two estimates from the true threshold will be much smaller than the difference of the two estimates.

In short, for sufficiently large ℓ, the finite-size effect should be significantly smaller than both the error tolerance and the difference of the two error estimates. We therefore only need to perform one simulation at an appropriately large value of ℓ for each (f,λ) pair. This computational technique was also used to measure the percolation threshold on the lattice [5]. Using only one value of ℓ also saves considerable computational resources in measuring the percolation threshold.

To obtain the error tolerance of 5×10^{-5} using a 400-MHz microcomputer, each value took between 3 and 215 h of computer time to generate the 0.3 to 1.5 billion arcs on each frontier. The computational burden increased significantly for large f and small λ. All told, about 56 billion arcs were generated over 13 weeks of computer time.

In Tables I and II, we present estimates of $\phi_c(f,\lambda)$ for various values of f and λ. These reported values are the averages of the two estimates $\phi_c^{(1)}(\ell)$ and $\phi_c^{(2)}(\ell)$, where ℓ is chosen so that these two estimates are within 7×10^{-5} of each other (and, in fact, are often closer). We see that all values are greater than the monodisperse threshold $\phi_c \approx 0.676\,339$, in agreement with the conjecture mentioned in the introduction. We also see that percolation thresholds much larger than ϕ_c can be achieved with appropriate choices for f and λ. The largest value of $\phi_c(f,\lambda)$ found in this study is

$$\phi_c(0.99,0.1) = 0.759\,81(5), \qquad (15)$$

and we conjecture that higher thresholds can be achieved at appropriate choices of f with smaller values of λ. In fact, for small λ, it appears that $\phi_c(f,\cdot)$ is maximized near $f=1-\lambda^2$.

TABLE II. Estimates of the percolation threshold $\phi_c(f,\lambda)$ for small λ and f close to 1. Again, each value has an estimated error of 5 in the last decimal place.

	$f=0.92$	$f=0.95$	$f=0.96$	$f=0.97$	$f=0.98$	$f=0.985$	$f=0.99$	$f=0.992$	$f=0.995$	$f=0.998$	$f=0.999$
$\lambda=0.1$	0.70027	0.71313	0.72064	0.73120	0.74643	0.75504	0.75981	0.75799	0.74570	0.71402	0.69718
$\lambda=0.2$	0.71929	0.72647	0.72746	0.72607	0.72010	0.71423	0.70564	0.70116	0.69329	0.68387	0.68007
$\lambda=0.3$	0.70876	0.70581	0.70333	0.69967	0.69412		0.68671		0.68195		
$\lambda=0.4$		0.69082			0.68387						
$\lambda=0.5$		0.68324			0.67958						

The data, presented as functions of f for selected values of λ, is also plotted in Fig. 2. The bottom axis corresponds to the monodisperse threshold. We observe that the maximum value of $\phi_c(\cdot,\lambda)$ increases as λ tends to zero and is achieved for values of f close to 1; this behavior was conjectured by Dhar [13]. We also note in passing that the results for $\lambda=0.9$ are not as smooth as the results for smaller λ. This occurs because the deviation of $\phi_c(f,0.9)$ from ϕ_c is on the order of the error tolerance.

B. Empirical formula

While it would be desirable to find an explicit formula for $\phi_c(f,\lambda)$ or find some kind of governing differential equation, such efforts appear to be difficult at best. Instead, we present here an empirical formula for $\phi_c(f,\lambda)$ based on the simulated values in Tables I and II. This empirical formula is found in terms of the *number density* of the larger disks, which may be given as

$$\rho_c'(f,\lambda)R^2=(1-f)\frac{-\ln\phi_c(f,\lambda)}{\pi[f\lambda^2+(1-f)]}.\tag{16}$$

Clearly $\rho_c'(0,\lambda)R^2\equiv\rho_c R^2\approx0.359\,072$, the number density of monodisperse disks [2]. Also, it is clear on physical grounds

that $\rho_c'(f,\lambda)<\rho_c$ for $f>0$; for such systems, the large disks by themselves are not sufficient to achieve percolation. Another boundary condition that must be obeyed is $\rho_c'(1,\lambda)=0$; again, we ignore the degenerate case $f=1$ and $\lambda=0$.

In Fig. 3, we show $\rho_c'(f,\lambda)/\rho_c$ as a function of f for selected values of λ. We see that, for each λ, the data may be well approximated using hyperbolas

$$\frac{\rho_c'(f,\lambda)}{\rho_c}\approx\frac{a(1-f)}{a-f},\tag{17}$$

where a is some parameter that depends on λ. By directly fitting data for $0.1\leqslant\lambda\leqslant0.9$, a reasonable empirical formula for a is

$$a=1+\frac{e^{6.8\lambda}}{115}.\tag{18}$$

While this empirical formula is satisfactory for $0.1\leqslant\lambda\leqslant0.9$, it does not satisfy the necessary limiting requirements. As $\lambda\to1$, we expect the number density of the ''bigger'' disks to approach $(1-f)\rho_c$. This occurs in Eq. (17) as $a\to\infty$. On the other hand, as $\lambda\to0$, the small disks should not contribute much at all to the percolation behavior. Therefore, we expect ρ_c' to remain close to ρ_c even for moderately large

FIG. 2. Estimates of the percolation threshold $\phi_c(f,\lambda)$ for binary dispersions. The bottom axis corresponds to the percolation threshold ϕ_c for disks of equal radius; this value is conjectured to be the smallest possible percolation threshold for disks. For small λ, the function $\phi_c(f,\lambda)$ is maximized for $f\approx1-\lambda^2$.
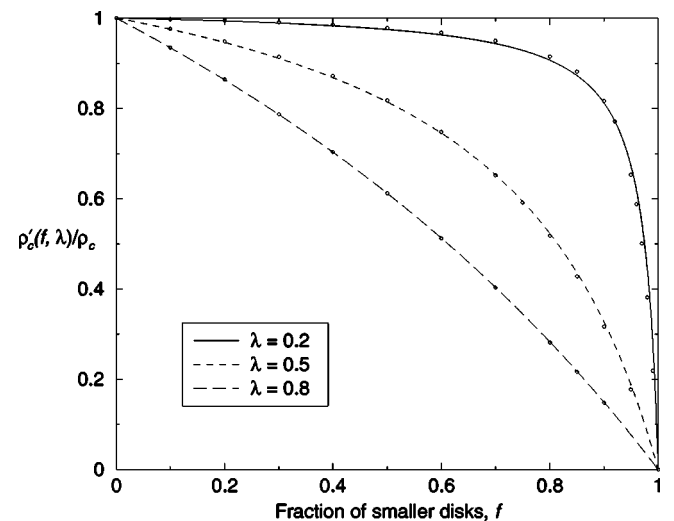
FIG. 3. Estimates of $\rho_c'(f,\lambda)/\rho_c$, as obtained from simulations for selected values of λ, are shown in circles. The hyperbolas are approximations of the form $a(1-f)/(a-f)$, where a is given by Eq. (18). These appear to be a reasonable empirical fit to the data.

values of f. However, ρ'_c must drop to its boundary value of 0 at $f = 1$. Thus, for small λ, the graph of ρ'_c should be very angled; this occurs in Eq. (17) as $a \to 1^+$.

We do not claim that Eq. (17) is exact or a rigorous approximation to the true number density of the large disks at percolation; it is only claimed to be a reasonable empirical fit to the data for $0.1 \leq \lambda \leq 0.9$. We also note in passing that, with this approximation, the percolation threshold itself may then be estimated by using Eqs. (16) and (17).

As mentioned in the Introduction, there has not been much study of the percolation threshold for disks of variable radii. One exception is the work of Dhar [13], who used a correlation-length argument for $\lambda \approx 0$ to derive the estimate

$$\rho_c(f,\lambda)R^2 \equiv \frac{\rho'_c(f,\lambda)R^2}{1-f} \approx x_c \frac{f\lambda^2 + 1 - f}{f\lambda^2 + (1-f)\lambda^{3/4}}, \quad (19)$$

where x_c is a constant. However, this estimate does not agree with our data for disks whose radii are within an order of magnitude of each other.

C. Fractal dimension and the Grossman-Aharony effect

The fractal dimension D_f of the frontier is computed by investigating the power-law behavior of the perimeter P and width σ of the frontier as a function of ℓ. The calculation of P and σ from the simulated frontier is given in Ref. [4]. Because the frontier is scaled to fit inside the unit square and the effective system length is inversely proportional to the gradient of the concentration, we note that

$$P \propto \ell^{\alpha_N} \text{ and } \sigma \propto \ell^{\alpha_\sigma - 1}, \quad (20)$$

where α_N and α_σ are the analogous critical exponents in previous percolation studies [11,14]. The fractal dimension of the frontier is related to these two exponents via

$$\alpha_N = (D_f - 1)\alpha_\sigma. \quad (21)$$

To ascertain power-law behavior, several simulations of ℓ are required for each (f,λ) pair. By contrast, only one value of ℓ was needed to accurately measure the percolation threshold. Therefore, the results of this section are not as exhaustive as our measurements of $\phi_c(f,\lambda)$. We choose to
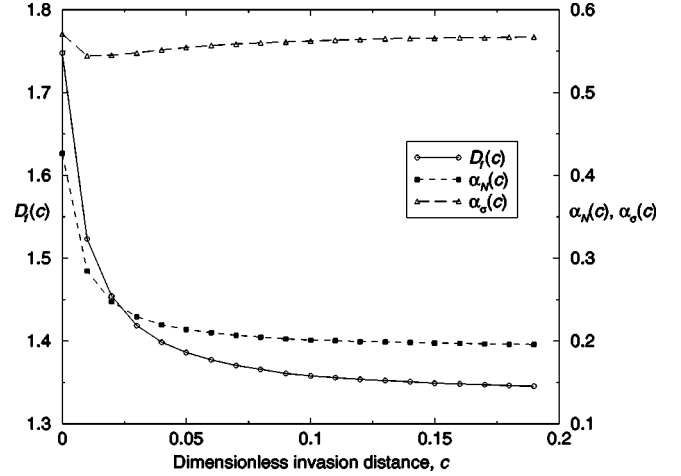
FIG. 4. Variation of the exponents $\alpha_N(c)$ and $\alpha_\sigma(c)$ and the fractal dimension $D_f(c)$ for $f = 0.6$ and $\lambda = 0.4$. Both $D_f(c)$ and α_N decrease rapidly to limiting values of approximately 4/3 and 1/5, respectively, while $\alpha_\sigma(c)$ remains nearly constant after an initial decrease.

measure the fractal dimension of the hull for $(f,\lambda) = (0.6,0.4)$, $(0.4, 0.8)$, $(0.8,0.2)$ and $(0.2,0.9)$.

For each frontier, we also simulate the *accessible* portion of the frontier. To do so, after simulating the frontier, the radius of each disk on the frontier — small and large — is increased by a small amount cR. This procedure closes small openings in the frontier to "invading" particles of radius $2cR$. A new front is then constructed as before, and the radius-dependent quantities $\alpha_N(c)$, $\alpha_\sigma(c)$, and $D_f(c)$ are also computed.

Our results for $(f,\lambda) = (0.6,0.4)$ are shown in Fig. 4; the graphs for the other choices of (f,λ) are similar. This figure is analogous to Fig. 4 of Ref. [14]. We see that binary dispersions exhibit the Grossman-Aharony effect [15,16] in precisely the same manner as monodisperse systems. We observe that $D_f(c)$ rapidly decreases from roughly 1.75 to 1.33 as c increases from 0. We also observe that $\alpha_\sigma(c)$ slowly increases after an initial decrease, while $\alpha_N(c)$ rapidly decreases to a limiting value of approximately 0.2. We conclude that diameter disorder has little to no effect on the fractal dimension.

[1] K. R. Mecke, in *Statistical Physics and Spatial Statistics*, edited by K. R. Mecke and D. Stoyan (Springer, New York, 2000).

[2] J. Quintanilla, S. Torquato, and R. M. Ziff, J. Phys. A **33**, L399 (2000).

[3] D. Stoyan, W. S. Kendall, and J. Mecke, *Stochastic Geometry and Its Applications*, 2nd ed. (Wiley, New York, 1995).

[4] J. Quintanilla and S. Torquato, J. Chem. Phys. **111**, 5947 (1999).

[5] R. M. Ziff and B. Sapoval, J. Phys. A **19**, L1169 (1986).

[6] M. K. Phani and D. Dhar, J. Phys. A **17**, L645 (1984).

[7] B. Lorenz, I. Orgzall, and H.-O. Heuer, J. Phys. A **26**, 4711 (1993).

[8] R. Meester, R. Roy, and A. Sarkar, J. Stat. Phys. **75**, 123 (1994).

[9] J. Quintanilla and S. Torquato, Phys. Rev. E **55**, 1558 (1997).

[10] J. A. Rice, *Mathematical Statistics and Data Analysis*, 2nd ed. (Duxbury, Belmont, CA, 1994).

[11] B. Sapoval, M. Rosso, and J. F. Gouyet, J. Phys. (France) Lett. **46**, L149 (1985).

[12] H. Saleur and B. Duplantier, Phys. Rev. Lett. **58**, 2325 (1987).

[13] D. Dhar, Physica A **242**, 341 (1997).

[14] M. Rosso, J. Phys. A **22**, L131 (1989).

[15] T. Grossman and A. Aharony, J. Phys. A **19**, L745 (1986).

[16] P. Meakin and F. Family, Phys. Rev. A **34**, 2558 (1986).